ISSN 1674-1056
http://cpb.iphy.ac.cn
http://iopscience.iop.org/cpb
中国物理 B
Chinese Physics
中国物理 Chinese Physics B

Negative transconductance effect in p-GaN gate AlGaN/GaN HEMTs by traps in unintentionally doped GaN buffer layer

Mei Ge(葛梅)[1], Qing Cai(蔡青)[1], Bao-Hua Zhang(张保花)[2], Dun-Jun Chen(陈敦军)[1], Li-Qun Hu(胡立群)[1], Jun-Jun Xue(薛俊俊)[3], Hai Lu(陆海)[1], Rong Zhang(张荣)[1], You-Dou Zheng(郑有炓)[1]

Citation: Chin. Phys. B . 2019, 28(10): 107301 . **doi:** 10.1088/1674-1056/ab3e00
Journal homepage: http://cpb.iphy.ac.cn; http://iopscience.iop.org/cpb

What follows is a list of articles you may be interested in

Method of evaluating interface traps in Al_2O_3/AlGaN/GaN high electron mobility transistors

Si-Qin-Gao-Wa Bao(包斯琴高娃), Xiao-Hua Ma(马晓华), Wei-Wei Chen(陈伟伟), Ling Yang(杨凌), Bin Hou(侯斌), Qing Zhu(朱青), Jie-Jie Zhu(祝杰杰), Yue Hao(郝跃)

Chin. Phys. B . 2019, 28(6): 067304 . **doi:** 10.1088/1674-1056/28/6/067304

Short-gate AlGaN/GaN high-electron mobility transistors with BGaN buffer

Tie-Cheng Han(韩铁成), Hong-Dong Zhao(赵红东), Xiao-Can Peng(彭晓灿)

Chin. Phys. B . 2019, 28(4): 047302 . **doi:** 10.1088/1674-1056/28/4/047302

Theoretical analytic model for RESURF AlGaN/GaN HEMTs

Hao Wu(吴浩), Bao-Xing Duan(段宝兴), Luo-Yun Yang(杨珞云), Yin-Tang Yang(杨银堂)

Chin. Phys. B . 2019, 28(2): 027302 . **doi:** 10.1088/1674-1056/28/2/027302

1.8-kV circular AlGaN/GaN/AlGaN double-heterostructure high electron mobility transistor

Sheng-Lei Zhao(赵胜雷), Zhi-Zhe Wang(王之哲), Da-Zheng Chen(陈大正), Mao-Jun Wang(王茂俊), Yang Dai(戴扬), Xiao-Hua Ma(马晓华), Jin-Cheng Zhang(张进成), Yue Hao(郝跃)

Chin. Phys. B . 2019, 28(2): 027301 . **doi:** 10.1088/1674-1056/28/2/027301

Characteristics and threshold voltage model of GaN-based FinFET with recessed gate

Chong Wang(王冲), Xin Wang(王鑫), Xue-Feng Zheng(郑雪峰), Yun Wang(王允), Yun-Long He(何云龙), Ye Tian(田野), Qing He(何晴), Ji Wu(吴忌), Wei Mao(毛维), Xiao-Hua Ma(马晓华), Jin-Cheng Zhang(张进成), Yue Hao(郝跃)

Chin. Phys. B . 2018, 27(9): 097308 . **doi:** 10.1088/1674-1056/27/9/097308

Negative transconductance effect in p-GaN gate AlGaN/GaN HEMTs by traps in unintentionally doped GaN buffer layer*

Mei Ge(葛梅)[1], Qing Cai(蔡青)[1], Bao-Hua Zhang(张保花)[2], Dun-Jun Chen(陈敦军)[1,†], Li-Qun Hu(胡立群)[1], Jun-Jun Xue(薛俊俊)[3], Hai Lu(陆海)[1], Rong Zhang(张荣)[1], and You-Dou Zheng(郑有炓)[1]

[1] *The Key Laboratory of Advanced Photonic and Electronic Materials, School of Electronic Science and Engineering, Nanjing University, Nanjing* 210093, *China*

[2] *Department of Physics, Changji College, Changji* 831100, *China*

[3] *School of Electronic Science and Engineering, Nanjign University of Posts and Telecommunications, Nanjing* 210023, *China*

(Received 6 May 2019; revised manuscript received 20 August; published online 30 September 2019)

We investigate the negative transconductance effect in p-GaN gate AlGaN/GaN high-electron-mobility transistor (HEMT) associated with traps in the unintentionally doped GaN buffer layer. We find that a negative transconductance effect occurs with increasing the trap concentration and capture cross section when calculating transfer characteristics. The electron tunneling through AlGaN barrier and the reduced electric field discrepancy between drain side and gate side induced by traps are reasonably explained by analyzing the band diagrams, output characteristics, and the electric field strength of the channel of the devices under different trap concentrations and capture cross sections.

Keywords: AlGaN/GaN, high-electron-mobility transistors (HEMTs), traps, negative transconductance

PACS: 73.40.Kp, 85.30.De, 85.30.Tv **DOI:** 10.1088/1674-1056/ab3e00

1. Introduction

Gallium nitride (GaN) high-electron-mobility transistors (HEMTs) are attractive for high-frequency, high-power semiconductor devices and sensor applications due to their high breakdown field, high mobility, and good thermal stability.[1,2] However, conventional AlGaN/GaN HEMTs are inherently normally-on devices because of a large amount of two-dimensional (2D) electron gas (2DEG) existing at the AlGaN/GaN interface.[3] In high-power applications with simple circuitry and system reliability, normally-off devices are highly desirable.[4] The structure with p-GaN cap layer can obtain normally-off performance by depleting the 2DEG in the interface, and has drawn increasing attention in the industry due to its large threshold voltage and low on-state resistance.[5–8]

The performances of GaN-based HEMTs can be limited by the presence of surface, bulk, and interface trap states.[9,10] More recently, the traps in the intentionally iron-doped GaN buffer layer have been studied to improve the performances of the GaN-based HEMTs.[11–13] However, little attention has been paid to the traps in the unintentionally-doped (UID) GaN buffer layer. Gallium nitrides are characterized by a high-density dislocations and several undesired impurities, complexes, and point defects. Therefore, there are intrinsic trap levels in the UID GaN buffer, which may have different effects on GaN-based HEMTs.[14] Negative transconductance means the decrease in drain current at a large gate voltage, and can be affected by these traps. Earlier researches have revealed the mechanisms of negative transconductance, such as the increase of the intrinsic base resistance in AlGaAs/GaAs HBTs,[15] the electric field distribution in the channel in HFETs,[16] surface-roughness in MOSFETs,[17] and electrode space in MIS tunnel diode.[18] And more recently, negative transconductance were found in MoS_2/Wse_2 heterojunction transistor.[19] However, few studies reported that the negative transconductance is attributed to the traps in UID buffer layer in p-GaN gate AlGaN/GaN HEMT.

In this paper, using the TCAD simulation we obatin transfer curves of the p-GaN gate AlGaN/GaN HEMTs, and find that high concentration and cross-section of traps in UID GaN buffer layer can result in negative transconductance of the device. Energy band diagrams, output curves, and electric filed distribution of the device are simulated to further study the mechanisms of negative transconductance.

2. Device characteristics

The TCAD device simulator based on ATLAS was used to model the device characteristics. Poisson's equation and continuity equation were applied to the numerical procedures. Newton iteration method was used to solve the nonlinear algebraic system equations until self-consistence was reached. We used the Schockley–Read–Hall recombination to model

*Project supported by the National Key Research and Development Program of China (Grant No. 2017YFB0402900), the National Natural Science Foundation of China (Grant No. 61634002), the Scientific Research Foundation of Graduate School of Nanjing University, China (Grant No. 2016CL03), and the Key Project of Jiangsu Province, China (Grant No. BE2016174).

†Corresponding author. E-mail: djchen@nju.edu.cn

© 2019 Chinese Physical Society and IOP Publishing Ltd

the traps.[20] Polarization model was taken into account due to the strong spontaneous and piezoelectric polarization effects in nitride semiconductors.[21] A low field mobility model and a nitride-specific high field dependent mobility model were used to consider various types of scattering mechanisms.[22] Fowler–Nordheim tunneling model was used to treat the tunnel effect.[23]

Figure 1 shows the schematic cross section of the proposed p-GaN gate AlGaN/GaN HEMT. The device consists of a 50-nm-thick p-GaN layer with an active hole density of 3×10^{17} cm^{-3}, a 15-nm-thick AlGaN layer with the Al mole fraction of 0.23, and a 2-μm-thick UID GaN buffer layer with a background carrier concentration of 1×10^{16} cm^{-3}. The acceptor trap energy level in the UID GaN buffer layer was set to be 0.4 eV below the conduction band minimum with adjustable concentrations and electron and hole capture cross sections, which are oftentimes detected in undoped GaN layers grown by MBE, particularly, under N-rich conditions.[24] The structure of the device is based on the experimental structure,[25] and the gate is assumed to be schottky contact, source and drain are assumed to be ohmic contacts. The gate–source distance is 1 μm, the gate–drain distance is 6 μm, and the width of the gate is assumed to be 1 mm.

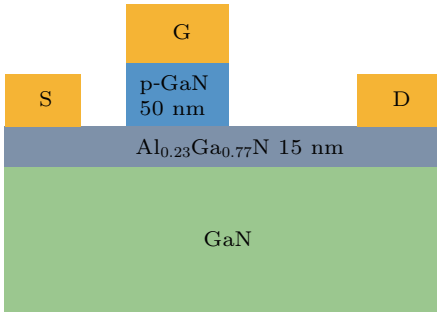


Fig. 1. Schematic cross section of the proposed p-GaN gate AlGaN/GaN HEMT.

As earlier paper reported, trap concentration in UID GaN buffer can be higher than 1×10^{17} cm^{-3} when the UID GaN buffer layer was grown by MOCVD at lower growth rate.[26] To characterize the effect of trap concentration in the UID GaN buffer layer on the negative transconductance of the devices, five trap concentrations are selected to be 1×10^{17} cm^{-3}, 3×10^{17} cm^{-3}, 5×10^{17} cm^{-3}, 7×10^{17} cm^{-3}, and 9×10^{17} cm^{-3}. The capture cross section is set to be 1×10^{-15} cm^2 in this case. Figure 2 shows the V_G–I_D curves of the devices with the five trap concentrations, where V_D is 10 V, and V_G is scanned from 0 V to 10 V in steps of 0.5 V. The threshold voltage of the devices is about 1.8 V. Normally, the drain current of the devices increases with the increase of gate voltage, and then is saturated when the gate voltage is large enough as indicated by the black and red curves in Fig. 2. However, as we can see in Fig. 2, the drain current drops when gate voltage is higher than 5 V and simultaneously the trap concentration reaches 5×10^{17} cm^{-3}, leading to a negative transconductance phenomenon. Therefore, concentration of traps in the UID GaN buffer layer is associated with negative transconductance of p-GaN gate AlGaN/GaN HEMTs.

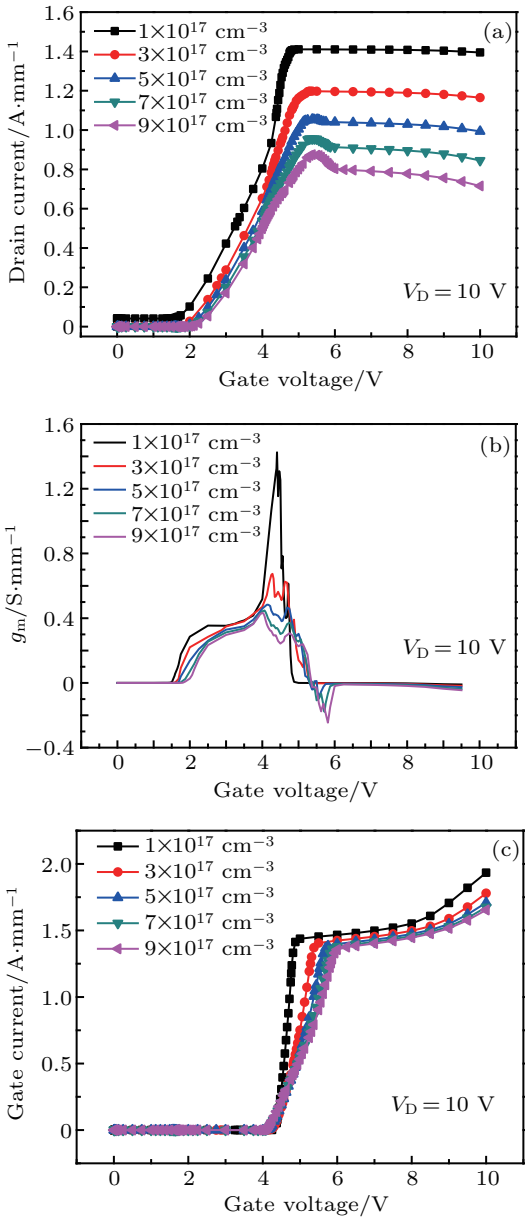


Fig. 2. (a) Transfer characteristics, (b) transconductance, and (c) I_G–V_G curves of devices, whereas trap concentrations are 1×10^{17} cm^{-3}, 3×10^{17} cm^{-3}, 5×10^{17} cm^{-3}, 7×10^{17} cm^{-3}, and 9×10^{17} cm^{-3}, and V_D is 10 V.

Figure 3 shows the transfer characteristics of the devices with four capture cross sections, which are set to be 1×10^{-16} cm^2, 1×10^{-15} cm^2, 1×10^{-14} cm^2, and 1×10^{-13} cm^2,[24] where V_D is 10 V, and V_G is scanned from 0 V to 10 V in steps of 0.5 V. We set the trap concentration to be 3×10^{17} cm^{-3} in this case. As shown in Fig. 3, the threshold voltage is about 1.8 V. When the capture cross section reaches 1×10^{-14} cm^2, the drain current drops at a gate voltage of about 5 V, leading to the negative device transconductance. Therefore, the capture cross section is also associated with

the negative transconductance of the p-GaN gate AlGaN/GaN HEMT.

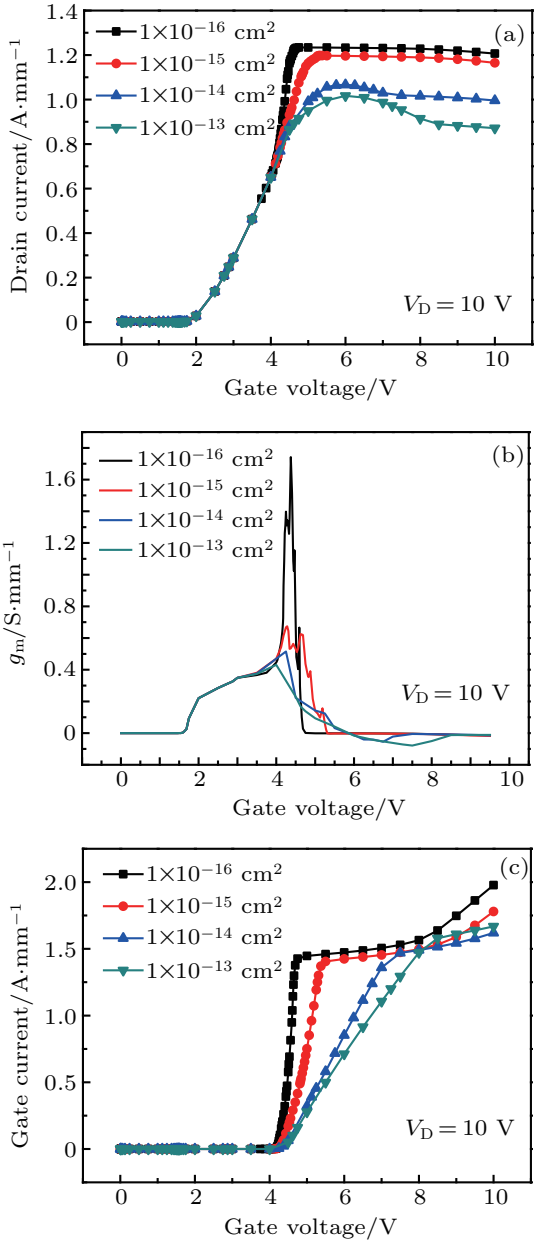


Fig. 3. (a) Transfer characteristics, (b) transconductance, and (c) I_G–V_G curves of the devices, whereas trap capture cross sections are 1×10^{-16} cm^2, 1×10^{-15} cm^2, 1×10^{-14} cm^2, and 1×10^{-13} cm^2, and V_D is 10 V.

3. Results and discussion

Traps in the UID GaN buffer layer are assumed to be acceptor-type traps which are unionized at zero gate bias, and they can ionize and capture electrons, with gate bias applied. This will influence the density and mobility of electrons in the channel, and hence influence drain current of device. In addition, electrons tunneling through the thin AlGaN barrier layer at a large gate bias can also influence the drain current. Drop in drain current at the large gate voltage means the occurrence of a negative transconductance phenomenon. In order to analyze the negative transconductance phenomenon associated with trap concentrations and capture cross sections as shown in Figs. 2 and 3, we provide the band diagrams, output characteristics of the device, and electric field distribution. Figure 4 shows the conduction band diagrams of the devices with the five trap concentrations at a gate voltage of 5 V. The device is open at this status and electrons are collected in the AlGaN/GaN interface. Triangle barrier forms at AlGaN layer, and electrons have possibility to tunnel through the AlGaN layer. As shown in Fig. 4(a), the triangle barrier becomes thinner with the increase of trap concentration, which makes it easier for the electrons in the potential well to tunnel through the AlGaN layer. These electrons can be attracted to the gate side and thus cause the gate current to increase as shown in Fig. 2(c). As a result, the electron density in the channel decreases with trap concentration increasing as shown in Fig. 4(b), and then results in a reduced drain current. Therefore, when trap concentration comes to a certain value, the negative transconductance phenomenon occurs.

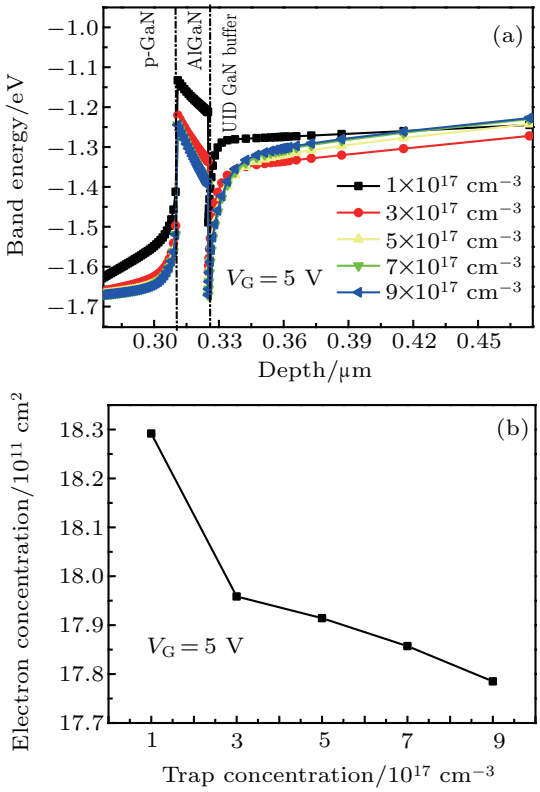


Fig. 4. (a) Band diagrams with five different trap concentrations. (b) Electron concentrations in channel. Gate voltage is set to be 5 V.

Figure 5(a) shows the output characteristics of the devices with the five different trap concentrations, with V_G being 5 V, and V_D being scanned from 0 V to 35 V. Because tunnel effect can influence the density of electrons in the channel as shown in Fig. 4, the drain current in the saturation region increases with the decrease of trap concentration. Figure 5(b) shows the variations of R_{on} value with trap concentration of the device calculated in the linear region of I_D–V_D curve for the five different trap concentrations, and we can see that the R_{on} increases with the increase of the trap concentration.

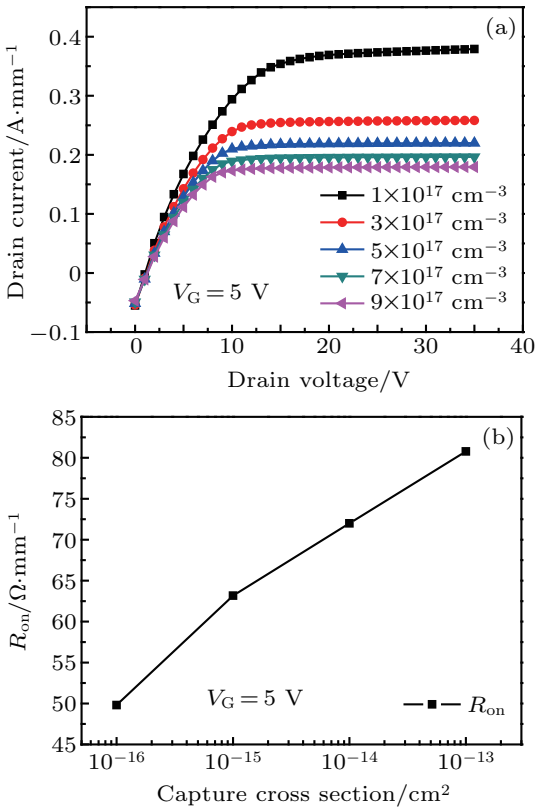


Fig. 5. (a) Output characteristics of devices with five different trap concentrations when $V_G = 5$ V. (b) Variations of R_{on} with trap concentration of devices with five trap concentrations calculated from curves in panel (a).

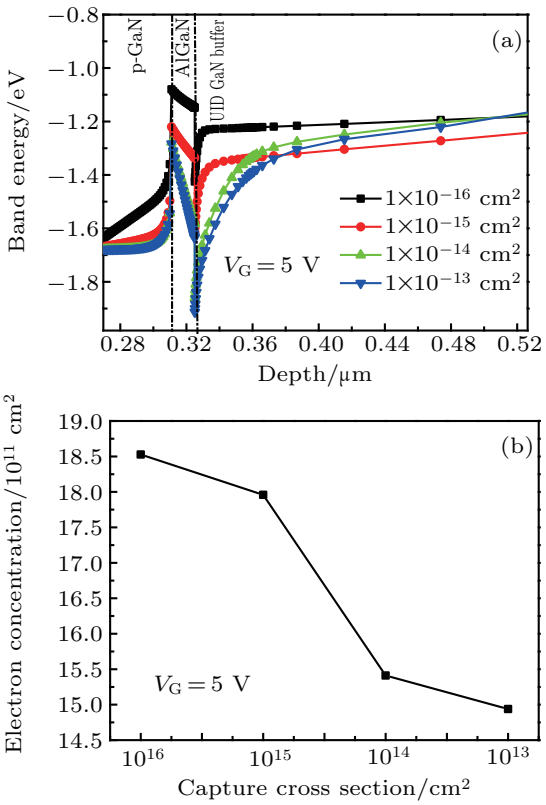


Fig. 6. (a) Band diagrams with the four different trap cross sections. (b) Electron concentrations in channel, with gate voltage being set to be 5 V.

Similarly, figure 6(a) shows the conduction band diagrams of the devices with the four capture cross sections at a gate voltage of 5 V. It can be seen that the triangle barrier becomes thinner with the increase of the capture cross section and makes the tunnel process of electrons take place easier, which will reduce electron concentration in the channel as shown in Fig. 6(b). These electrons can be attracted to the gate side and cause the gate current to increase as shown in the Fig. 3(c). The calculated output characteristics of the devices show that the saturation current decreases with the increase of capture cross section as shown in Fig. 7(a). The R_{on} values of the devices, calculated from linear region of I_d–V_d curve, increases with the increase of the capture cross section as shown in Fig. 7(b).

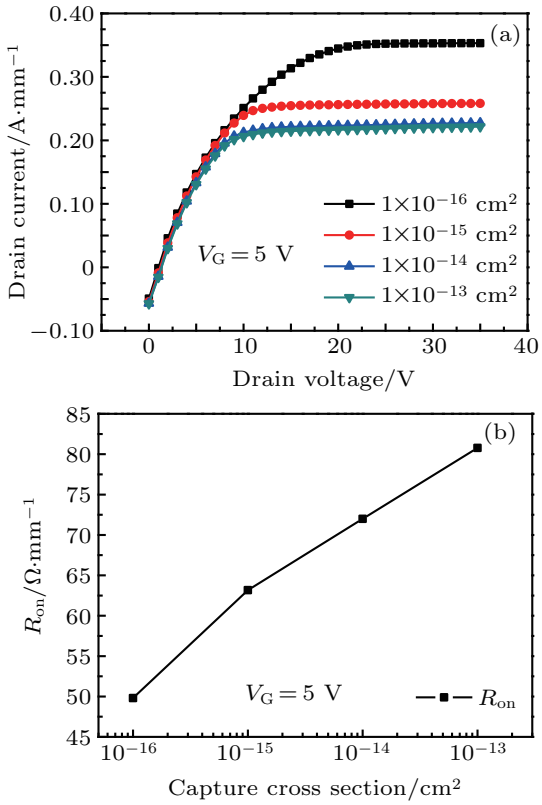


Fig. 7. (a) Output characteristics and (b) R_{on} of devices with different capture cross sections at $V_G = 5$ V.

The negative transconductance effect in the device can be attributed to the tunnel effect, which is related to the trap concentration and cross section in the UID GaN buffer layer as shown in Fig. 8. The tunneling is Fowler–Nordheim (FN) tunneling, and the tunneling probability can be expressed as[27]

$$T_{EN} = \exp\left[\frac{-4\sqrt{2md}}{2heV_{bias}}(E_F + \phi_E - E_z)^{3/2}\right],$$

where m is the electron mass, ϕ_F is the barrier height from E_F, d is the barrier width, and E_z is energy component of electrons normal to the barrier surface. The eV_{bias} is shown in Fig. 8. The value of eV_{bias} increases with trap concentration and trap cross section increasing as shown in Figs. 4(a) and 6(a), which results in a larger T_{FN}. And hence the electron concentration in the channel becomes smaller. Therefore, drain current drops at higher trap concentration and cross section.

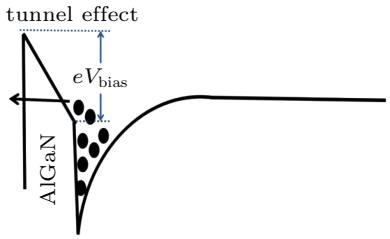


Fig. 8. Schematic diagram of tunnel effect resulting in negative transconductance.

Figure 9(a) shows the variations of electric field strength with gate voltageith at drain and gate side of the channel of the device with a trap concentration of 3×10^{17} cm^{-3} under different gate voltages. The values of V_G are set to be 5, 7, and 9 V, because the negative transconductance appears when V_G reaches 5 V as shown in Fig. 2. We can see from Fig. 9(a) that the value of electric field at drain side is higher than that at gate side with the increase of the gate voltage, but the difference between them decreases at higher gate voltage. Figure 9(b) shows the difference in electric field between drain side and gate side for the five trap concentrations, where V_G is 7 V. The difference in electric field between drain side and gate side decreases with trap concentration increasing. This decrease causes the difference in electron mobility between drain side and gate side to increase. Therefore, more carriers are attracted to the gate side with larger trap concentration, which leads the drain current to decrease. As a result, the reduced drain current at large trap concentration will cause a negative device transconductance as shown in Fig. 2.

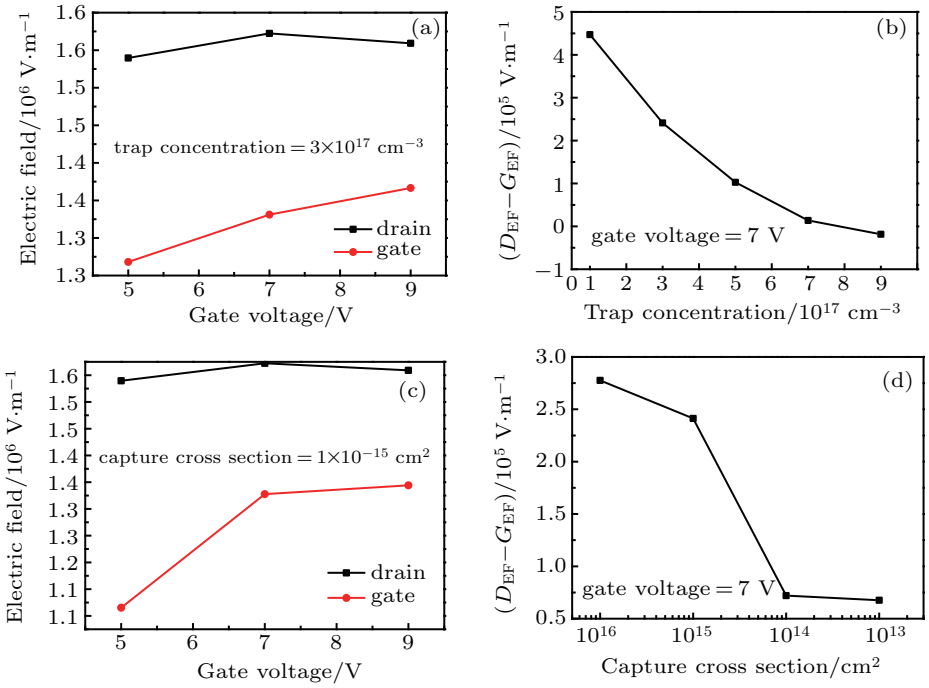


Fig. 9. Electric field strength at drain and gate sides of the channel of the device with (a) trap concentrations of 3×10^{17} cm^{-3} and (c) capture cross section of 1×10^{-15} cm^2 under different gate voltages. Difference in electric field between drain side and gate side for (b) five different trap concentrations and (d) four capture cross sections, with V_G being 7 V.

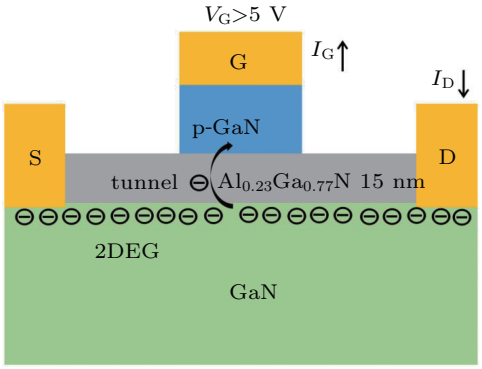


Fig. 10. Mechanism of negative transconductance, with $V_G > 5$ V.

Similarly, the difference in electron mobility between drain side and gate side decreases with capture cross section increasing, which leads the drain current to decrease, which finally gives rise to the negative transconductance effect.

In conclusion, when gate voltage reaches 5 V, more electrons are attracted to the gate side at higher trap concentration and capture cross section, which results in a decrease of drain current and an increase of gate current as shown in Fig. 10.

4. Conclusions

In this paper we study the negative transconductance effect in p-GaN gate AlGaN/GaN HEMTs that is associated with traps in the unintentionally doped GaN buffer layer. By simulation, we find that electrons are easier to tunnel through AlGaN barrier layer with increasing trap concentration and capture cross section, and simultaneously, the difference of electric field between drain side and gate side decreases. As a

result, drain current drops and hence results in the occurrence of negative transconductance effect. This phenomenon occurs when the trap concentration reaches 5×10^{17} cm^{-3} (whereas capture cross section is 1×10^{-15} cm^2) and capture cross section reaches 1×10^{-14} cm^2 (whereas trap concentration is 3×10^{17} cm^{-3}).

Acknowledgment

The authors thank colleagues of Prof. Chen Dunjun's group for their help.

References

[1] Frayssinet E, Knap W, Lorenzini P, Grandjean N, Massies J, Skierbiszewki C, Suski T, Grzegory I, Porowski S, Simin G, Hu X, Shur M S, Gaska R and Maude D 2000 *Appl. Phys. Lett.* **77** 2551
[2] Kuzuhara M and Tokuda H 2015 *IEEE Trans. Electron. Dev.* **62** 405
[3] Ambacher O, Foutz B, Smart J, Shealy J R, Weimann N G, Chu K, Murphy M, Sierakowski A J, Schaff W J, Eastman L F, Dimitrov R, Mitchell A and Stuzmann M 2000 *J. Appl. Phys.* **87** 334
[4] Su M, Chen C and Rajan S 2013 *Semicond. Sci. Technol.* **28** 074012
[5] Ťapajna M, Hilt O, Bahat T E, Wiirfl J and Kuzmik J 2016 *IEEE Electron Dev. Lett.* **37** 385
[6] Greco G, Iucolano F, Franco S D, Bongiorno C, Patti A and Roccaforte F 2016 *IEEE Trans. Electron. Dev.* **63** 2735
[7] Su L Y, Lee F and Huang J J 2014 *IEEE Trans. Electron. Dev.* **61** 460
[8] Rossetto I, Meneghini M, Hilt O, Bahat T E, Santi C D, Dalcanale S, Wuerfl J, Zanoni E, Meneghesso G 2016 *IEEE Trans. Electron. Dev.* **63** 2334
[9] Vetury R, Zhang N Q, Keller S and Mishra U K 2001 *IEEE Trans. Electron. Dev.* **48** 560
[10] Tirado J M, Sánchez R J L and Izpura J I 2007 *IEEE Trans. Electron. Dev.* **54** 410
[11] Heikman S, Keller S, DenBaars S P and Mishra U K 2002 *Appl. Phys. Lett.* **81** 439
[12] Uren M J, Moreke J and Kuball M 2012 *IEEE Trans. Electron. Dev.* **59** 3327
[13] Axelsson O, Gustafsson S, Hjelmgren H, Rorsman N, Blanck H, Splettstoesser J, Thorpe J, Roedle T and Thorsell M 2016 *IEEE Trans. Electron. Dev.* **63** 326
[14] Ge M, Cai Q, Zhang B H, Chen D J, Hu L Q, Xue J J, Lu H, Zhang R and Zheng Y D 2018 *Phys. Status Solidi A* **215** 1700368
[15] Nozu T and Obara M 1990 *J. J. Appl. Phys.* **29** 2376
[16] Baek J and Shur M 1990 *IEEE Trans. Electron. Dev.* **37** 1917
[17] Versari R and Ricco B 1999 *IEEE Trans. Electron. Dev.* **46** 1189
[18] Liao C S and Hwu J G 2016 *IEEE Trans. Electron. Dev.* **63** 2864
[19] Nourbakhsh A, Zubair A, Mildred S D and Palacios T 2016 *Nano Lett.* **16** 1359
[20] Schlichenmaier C, Thranhardt A, Meier T, Koch S W, Chow W W, Hader J and Moloney J V 2005 *Appl. Phys. Lett.* **87** 261109
[21] Guo B and Ravaioli U 2002 *J. Comput. Electron.* **1** 309
[22] Albrecht J D, Wang R P, Ruden P P, Farahm, M and Brennan K F 1998 *J. Appl. Phys.* **83** 4777
[23] Cai Q, Ge M, Xue J J, Hu L Q, Chen D J, Lu H, Zhang R and Zheng Y D 2017 *IEEE Photon. J.* **9** 6803507
[24] Polyakov A Y and Lee I H 2015 *Mater. Sci. Eng. R* **94** 1
[25] Erofeev E V, Kagadei V A, Kazimirov A I and Fedin I V 2015 *International Siberian Conference on Control and Communications*, May 21–23, 2015, Omsk, Russia
[26] Cho H K, Kim C S and Hong C H 2003 *J. Appl. Phys.* **94** 1485
[27] Nagahama T, Santos T S and Moodera J S 2007 *Phys. Rev. Lett.* **99** 016602